Lab on a Chip

PAPER

View Article Online
View Journal | View Issue

Cite this: *Lab Chip*, 2014, **14**, 4000

A continuous-flow *C. elegans* sorting system with integrated optical fiber detection and laminar flow switching†

Yuanjun Yan,[a] Li Fang Ng,[b] Li Theng Ng,[b] Kwan Bum Choi,[c] Jan Gruber,[b] Andrew A. Bettiol*[c] and Nitish V. Thakor[a]

Received 25th April 2014,
Accepted 7th August 2014

DOI: 10.1039/c4lc00494a

www.rsc.org/loc

We present a high-throughput continuous-flow *C. elegans* sorting device that works based on integrated optical fiber detection and laminar flow switching. Two types of genetically engineered nematodes are allowed to flow into the device and their genotypes are detected based on their fluorescence, without the need for immobilization, by integrated optical fibers. A novel dynamic fluidic switch sorts the nematodes to desired outlets. By changing input pressures of the control inlets, the laminar flow path is altered to steer the nematodes to appropriate outlets. Compared to previously reported microfluidic *C. elegans* sorting devices, sorting in this system is conducted in a continuous flow environment without any immobilization technique or need for multilayer mechanical valves to open and close the outlets. The continuous flow sorter not only increases the throughput but also avoids any kind of invasive or possibly damaging mechanical or chemical stimulus. We have characterized both the detection and the switching accuracy of the sorting device at different flow rates, and efficiencies approaching 100% can be achieved with a high throughput of about one nematode per second. To confirm that there was no significant damage to *C. elegans* following sorting, we recovered the sorted worms, finding no deaths and no differences in behavior and propagation compared to control.

Introduction

The nematode *Caenorhabditis elegans* is a model organism that is widely utilized for genetic, developmental and biochemical investigations.[1] Martin Chalfie first described the use of a green fluorescent protein (GFP) derived from jellyfish to monitor gene expression and protein localization in *C. elegans*.[2] GFP reporter gene constructs are generated by fusing the gene sequence coding for GFP either to a promoter fragment from a gene of interest or by gene fusions between GFP and a gene of interest.[3] Since they were first described, hundreds if not thousands of GFP reporter gene strains have been generated. A recent search for GFP strains in the *C. elegans* Genetics Centre (CGC) strain list reveals over 3800 GFP strains.[3] Such GFP strains have been developed and used for a wide range of purposes. They are routinely used for optical selection of genotypes and real-time *in vivo* determination of gene-product localization and temporal–spatial expression patterns.[2,4] In inducible signalling pathways, in-frame gene fusions between GFP and the gene of interest or similarly GFP-tagged transcription factors can be used to map pathways and determine tissue-specific gene expression levels under different conditions and developmental stages.[2,4,5] Another emerging class of applications is large-scale genetics or pharmacological screens.[6,7] When used in conjunction with deletion mutants, genome-wide RNA interference or chemical inhibitor libraries, such GFP reporter gene constructs can be used to determine gene epistasis and identify pharmacological inhibitors and activators. However, to fully realize the potential of these *C. elegans* tools, high-throughput technologies are required due to the intrinsic limitations of manual screening approaches in terms of scalability and reproducibility.[8] One commercially available system, the COPAS Biosort™,[9] is a high-throughput sorter that utilizes a traditional, capillary-based fluorescence-activated cell sorting (FACS) technology.[10] Although successfully implemented and used in different kinds of gene expression studies,[11,12] this system is challenging to run and maintain, and the prohibitively high cost has hindered its usage in most academic settings.[13]

In recent years, microfluidics has been widely used in different kinds of *C. elegans* studies.[14] Microfabrication makes it possible to mass-produce microfluidic devices with

[a] *Singapore Institute for Neurotechnology, 28 Medical Dr. #05-COR, Singapore 117456*
[b] *Yale-NUS College, 6 College Ave East, #B1-01, Singapore 138614*
[c] *Department of Physics, National University of Singapore, 2 Science Dr 3, Singapore 117542. E-mail: a.bettiol@nus.edu.sg*

† Electronic supplementary information (ESI) available. See DOI: 10.1039/c4lc00494a

optically transparent materials such as polydimethylsiloxane (PDMS). Enabled by microchannels to trap and guide the nematodes, microfluidic devices hold the potential for high-throughput *C. elegans* imaging, screening and behavioural investigations.[15–18] To overcome the limitations of manual sorting, such as time and labour demands as well as variability, bias and errors that are intrinsic with manual techniques, while avoiding the prohibitive costs of automatic sorters like COPAS, different groups have come up with several innovative sorting designs that are all based on microfluidics and fabricated with single or multiple patterned PDMS layers. In 2007, Rohde *et al.* designed a multilayer PDMS system that can automatically load, immobilize, image and sort *C. elegans*.[19] A thin PDMS membrane is controlled by air pressure and can be deformed to keep the nematodes from moving. In 2008, Chung *et al.* developed a similar system that uses local cooling to immobilize *C. elegans*.[20] After analysing the nematodes with various imaging techniques, several multilayer PDMS valves were designed to switch the worms to the desired outlets by blocking others.

In general, the majority of microfluidic-based *C. elegans* sorting systems have followed an "immobilization-imaging-release" approach. Different methods of immobilization have been utilized for this purpose, including a tapered channel design[16] and PDMS microvalves,[19,21] which fall into the category of mechanical immobilization, the above-mentioned cooling method,[20] and reduction of the nematodes' activities through the increase of CO_2 concentration.[22] These approaches permit the imaging of *C. elegans* only while their locomotion is partially or completely restrained. However, immobilization by these means can potentially be harmful to the worms with effects ranging from unintended activation of stress response pathways to injury and death. These effects may confound certain biological and behavioural studies, especially ageing and lifespan studies, which are known to be prone to such artefacts.[23] Furthermore, the immobilized detection significantly decreases the throughput and increases failure rate when trying to immobilize fast-moving nematodes. Therefore, immobilization should ideally be minimized.

Another drawback of most existing microfluidic sorters originates from their switching mechanism. The fabrication of PDMS valves requires sophisticated multilayer fabrication methods with repeated deformation of PDMS during actuation.[13,15] This places significant strains on the active components and 3D bonded elements of the chip, limiting the number of actuations that can be carried out before the chip fails. Such valve-based switching prevents real-life applications requiring the device to function continuously in order to handle thousands of worms, and hence explains why none of the systems described thus far have neither found broader appeal outside of the developers' labs nor been developed and offered commercially.

Here, we present a novel "worm-chip" with several innovations. First is an integrated optical system that utilizes two pairs of optical fibers to detect and differentiate *C. elegans* genotypes based on the difference in their optical signals as they swim through. The immobilization-free approach not only avoids potential stressful stimuli to the *C. elegans* nematodes but also increases the sorting throughput, as the flow need not be paused for imaging. Second, switching is achieved by dynamic control of the laminar flow fields without the need for three-dimensional multilayer soft lithography or spin-coated thin PDMS membranes as seen in prior studies,[20,22] making the fabrication easier and more straightforward. This novel approach guarantees an uninterrupted flow, which ensures a constant flow rate and makes the precise timing of the detection and switching possible, thus increasing the sorting accuracy. Furthermore, the constant flow significantly reduces the chance of clogging problems within the channels. Last but not least, having no active components within the chip makes the device more robust and durable: it can almost be used as a permanent sorting device. Our *C. elegans* sorting characterization demonstrates a 96.6% sorting accuracy at a sorting rate of around 1 s per worm without damaging them, allowing full recovery of sorted worms.

Experimental design

Microfluidic device structure

Fig. 1 illustrates the general design concept with the inset showing the microscopic photograph of the PDMS-based

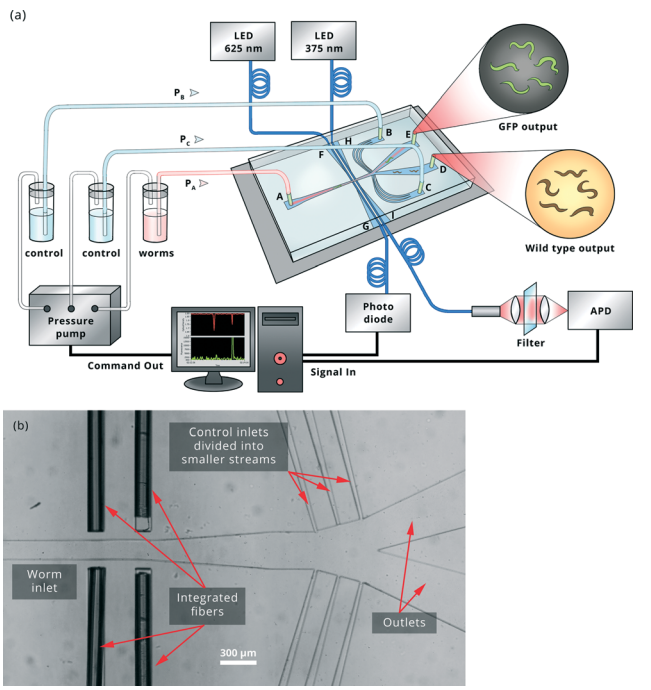

Fig. 1 (a) Schematic of the sorting device. It has one worm inlet (A), two buffer inlets (B, C), two outlets (D, E) and four optical fiber channels (F–I). The optical fibers emit and collect the light signals that are used to differentiate wild-type and GFP nematodes and transfer them to a computer, which writes commands to a pressure pump that is connected to the three inlets to create laminar flows in order to guide the worms to exit from the desired outlets; (b) optical image of the device with the fibers inserted in.

microfluidic worm sorter. The device consists of 5 channels: A (worm inlet), B and C (control inlets), D and E (outlets). In addition, 4 optical fiber inlets (F–I) are fabricated on both sides of the worm inlet. The whole chip is fabricated in a single-layer PDMS with standard soft lithography techniques and subsequently bonded to a glass slide. Pressure sources are connected to inlets A, B and C with pressures P_A, P_B and P_C, respectively, to drive the flows to exit from outlets D and E. The mixture of GFP-type and wild-type *C. elegans* nematodes enters the device from inlet A only. The inlet is gradually tapered to straighten the nematodes for detection. Optical fibers are inserted into channels F–I in order to detect and differentiate the genotypes. Based on the optical signals, P_B and P_C change accordingly to dynamically guide the nematodes to exit from the desired outlets. In order to prevent the *C. elegans* nematodes from exiting from inlet B or C, both the channels are divided into three 30 μm wide openings at the intersections that allow liquid flow but are too narrow for the adult *C. elegans* (typical width 60–100 μm) to pass through.

Detection mechanism

At the sides of the worm channel are two pairs of fiber inlets, each having a width of 125 μm and a height of 90 μm, which is the height of the chip. The schematic is illustrated in Fig. 2(a). Before insertion, the fibers are stripped down to 125 μm and cleaved to create a flat surface in order to reduce insertion loss. The cross section of the stripped fiber is slightly larger than the cross section of the fiber inlet; however, the fiber can still be inserted in after lubrication due to the elasticity of PDMS, as shown in Fig. 2(b). The slight deformation of PDMS does not affect the flow or cause any bonding problems.

Two pairs of fibers are used, with each pair consisting of an emitting fiber and a detection fiber opposing each other. The first pair signals the existence of a *C. elegans* nematode. The emitting fiber is connected to a 625 nm LED light source and the detection fiber is connected to a photodiode that is used to measure light intensity coming from the emitting fiber. When a nematode crosses the light path, light is partially absorbed due to the semitransparent nature of *C. elegans*. Also, as the worm and fiber core are not center-aligned in the vertical direction, the worm further diffracts the light out of the detection fiber core. The process is simulated with ray tracing software as shown in Fig. 2(c). Over 80% of the incident light is diffracted as the result shows. This results in a drop of the light intensity collected by the detection fiber that indicates the presence of a nematode. The second pair of fibers in this device determines the genotype. The emitting fiber is connected to a 375 nm LED light source and the detection fiber is connected to an avalanche photodiode (APD) that is able to measure low levels of green fluorescence from a GFP nematode. When a GFP nematode passes by, it will be excited by the UV light from the emitting fiber or alternatively by the microscope fluorescent lamp if the experiment is carried out on a microscope platform. Similarly as in the first pair, the second detection fiber collects green fluorescent signals from the excited GFP-type nematode. Since the excitation light is also captured, a laser line filter at 510 nm is used in front of the APD to allow only the fluorescent light to pass through. By combining the two sets of fibers, the system is capable of detecting the nematodes' existence and their genotypes, allowing us to do sorting as well as sample statistics such as worm counting.

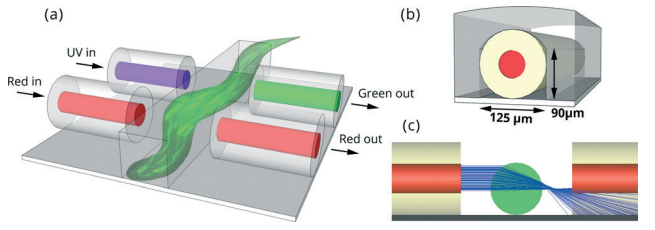

Fig. 2 (a) Illustration of the fiber detection scheme. When a worm passes through the detection region, it blocks part of the red light which is detected by the first pair of fibers. The second pair of fibers excites and detects the GFP fluorescence of the worm if applicable, further differentiating the worm type. (b) The cross-sectional schematic of the fiber inlets with 125 μm width and 90 μm height. When the fiber is inserted, PDMS will be slightly deformed without affecting bonding due to its elastic property. (c) Ray tracing confirms that with the existence of the worm, light is diffracted to give a significant drop of detected intensity.

Switching mechanism

Unlike the PDMS valve-based sorters, switching in this device is achieved by dynamically controlling the laminar flow fields, which is the main characteristic of the microfluidic chip. There are 3 inflows into the device: inflows A, B and C under pressures P_A, P_B and P_C, respectively. The inflows first merge in the device with no mixing due to laminar flow at the microscale and subsequently exit from outlets D and E. Thus, two clear flow boundaries will be observed and the positioning of which can be controlled by P_B and P_C with P_A kept constant. By adjusting P_B and P_C, it is possible to control how inflow A, which is the worm flow, exits from the two outlets.

To explore the switching mechanism, a COMSOL Multiphysics (COMSOL, Inc., MA 01803, USA) simulation was carried out and the results are presented in Fig. 3. Worm flow is denoted in red and buffer solution in blue. Under different pressure configurations, we have plotted the concentration distribution of the worm flow along the sorting device. The simulation indicates an unmixed laminar flow when the three streams merge. Furthermore, by changing pressures P_B and P_C the laminar flow boundaries can be moved, and consequently, the worm flow can be steered to exit completely or partially from either of the outlets. It is shown from the simulation graphs that a larger Δ results in better switching as the outflow from the unwanted outlet is minimized.

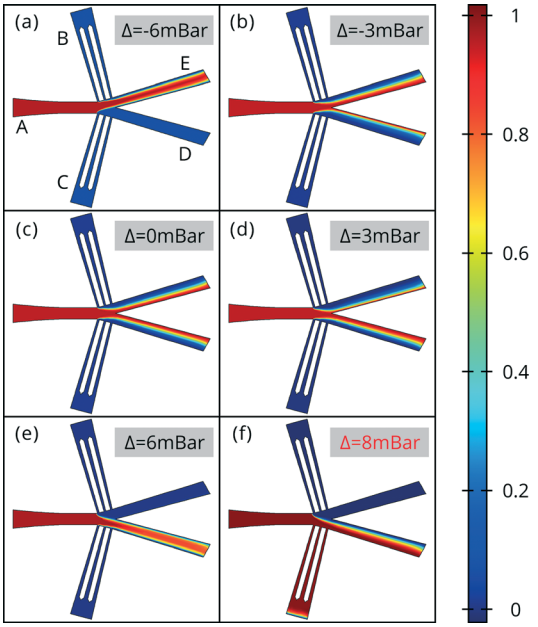

Fig. 3 COMSOL simulation of the laminar flow switching. Worm inflow is denoted in red and buffer solution in blue. Similar to the experiment, worms flow in from the left inlet A with pressure P_A = 20 mbar and buffer solutions from the top and bottom control inlets B and C. The difference of the two buffer pressures P_B and P_C is represented by Δ, and each of the plots shows the concentration of the worm flow along the whole sorting device. (a) P_B = 7 mbar and P_C = 13 mbar. With a −6 mbar difference, almost the whole worm inflow is steered to the top outlet; (b) when Δ is reduced to −3 mbar, the boundaries start to move towards the bottom outlet; (c) when equal pressures are exerted on the buffer inlets, the outflow is symmetrically distributed between the outlets; (d) further increase of Δ results in more movements of the laminar flow boundaries towards the bottom, until (e) almost the whole worm flow exits from the bottom outlet; (f) in an extreme case when Δ is too large, worm flow exits from the bottom control inlet.

However, Fig. 3(f) shows that a very large Δ may cause the nematodes to exit from the opposing control inlet. To solve this problem experimentally, each of the control inlets is further divided into three narrow streams with a width of 30 μm at the merging intersection. This size is small enough to stop the animals from entering the control inlets (as shown in Fig. 1(b)).

To demonstrate experimentally the laminar flow switching, we have carried out an experiment where blue dye is used to represent the worm inflow and water is used as the buffer solution. Snapshots are shown in Fig. 4 to clearly indicate that laminar flow switching occurs in agreement with COMSOL simulation results (see Video S1† for blue dye switching demonstration in real time).

Results and discussion

Worm detection with integrated optical fibers

As mentioned above, integrated fibers are used to detect and classify nematodes as they flow. In order to achieve a high signal-to-noise ratio, the fibers must be located as close to the channel and to each other as fabrication tolerances allow. On the other hand, if the channel is too narrow, clogging of the worms may occur. The optimized dimension that we use is a 90 μm channel at the detection area, with each fiber being 50 μm away from the channel. In addition, the 90 μm channel is gradually tapered down from 300 μm width at the inlet entrance. The advantage of gradually tapering the channel is twofold: firstly, it brings the fibers closer for a more accurate measurement; secondly, the 90 μm width is small enough to allow only one worm to pass through the detection region at a time, while being big enough to prevent any congestion. A typical detection event is shown in Fig. 5.

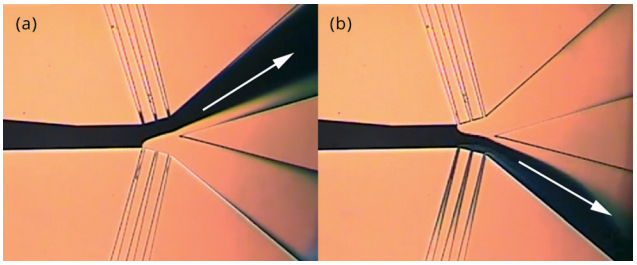

Fig. 4 Experimental demonstration of the laminar flow switching mechanism, in which blue dye is used as worm flow. (a) P_A = 20 mbar, P_B = 8 mbar and P_C = 12 mbar. This results in the blue dye exiting from the top outlet (outlet E in Fig. 1(a)); (b) P_B and P_C are swapped to result in switching to the opposite direction. Real-time switching is shown in Video S1.†

Automated fast switching of *C. elegans*

In order to sort *C. elegans* nematodes in a fast and automated manner, we have developed a software program to automatically detect and switch wild-type and GFP genotypes (implemented in LabVIEW, National Instruments). Fig. 6 illustrates the sorting process. The default pressure configuration is P_B = 20 mbar and P_C = 0. In this configuration, the

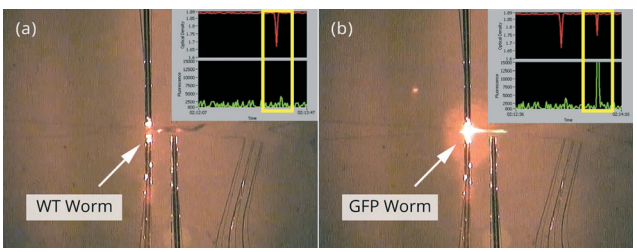

Fig. 5 Passage of worm by the optical fibers and the detected signals of (a) a wild-type worm and (b) a GFP worm. The insets show relative light intensity detected by the optical density detection fiber and green fluorescence detection fiber, denoted in red and green, respectively. In scenario (a), when the wild-type worm passes by the fibers it diffracts the red light while giving out no green fluorescence. As a result, a signal dip is shown for the optical density measurement and no observable signal for GFP measurement is seen. In scenario (b), when the GFP worm passes by the fibers it not only diffracts the red light but also is excited to emit green fluorescence, as shown in the optical image. Consequently, the optical density detector shows a dip while the GFP detector shows a signal peak.

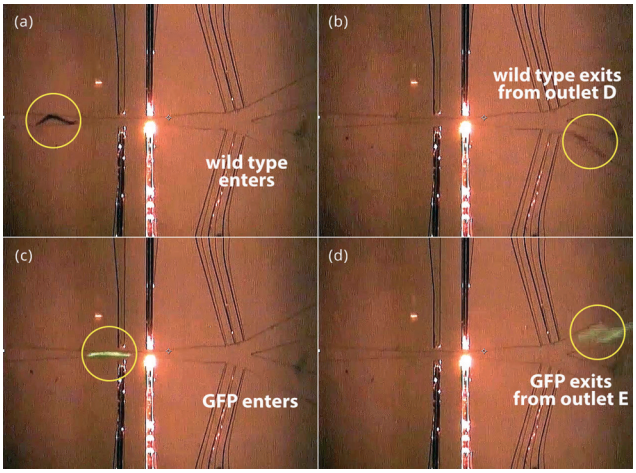

Fig. 6 Snapshots of (a–b) a wild-type worm and (c–d) a GFP worm being sorted by the device. Worms are circled in yellow. Note that since the sorting was carried out on a microscope platform, the excitation of GFP was achieved by the built-in fluorescent lamp and therefore the GFP excitation fiber was not inserted. In scenario (a–b), P_B = 20 mbar and P_C = 0, so the worm is steered to exit from bottom outlet D; in scenario (c–d), P_B = 0 and P_C = 20 mbar, therefore the worm is steered to exit from top outlet E. The switching takes place in milliseconds time that results in blurred snapshots of the worms. For a clearer view of the sorting process, refer to Video S2.†

device steers all animals to exit the device from the bottom outlet D. The worm inlet pressure P_A can also be changed to achieve different flow rates. The pressure difference between P_B and P_C (20 mbar) is large enough to give a high switching accuracy, and the 30 μm narrow openings ensure that no worms will be pushed into the opposing control inlets. Fig. 6a and b show how a wild-type worm flows in and out with the default pressure configuration. This pressure configuration will only be changed when a GFP worm is detected. In this case, both pairs of fiber will detect the signals as shown in the inset of Fig. 5(b), and the software will trigger pressures P_B and P_C to immediately swap (P_B = 0 and P_C = 20 mbar). It takes approximately 100 ms for a new laminar flow configuration to be set up resulting in the GFP worm exiting the device from the top outlet E, as shown in Fig. 6(c–d). For more details, refer to Video S2.† Since the experiment is carried out using a fluorescence microscope, GFP is excited with the fluorescent lamp; hence, the excitation fiber is not required. This device is, however, able to operate without a microscope and all the signals can be collected by optical fibers.

Pressure sorting accuracy characterization

The accuracy of a sorting device depends on both detection and switching. At low flow rates (typically <3 mm s^{-1}), the detectors and pressure pump are able to respond fast enough to each individual animal passing through the device. However, under such conditions, the throughput in terms of animals sorted per time is relatively low. When a high flow rate (>10 mm s^{-1}) is applied, it is possible for the device to miss some of the animals if they arrive in a short time period. In order to determine the highest throughput and the practical limit of the sorting device, we have characterized a mixture of around 500 wild-type and GFP worms mixed at a roughly 1 : 1 ratio in terms of genotype at a density of 40 ml^{-1}. The worms were pumped through the device at various flow rates. Various parameters were recorded including the genotype, speed, detection accuracy and sorting performance.

We found that fiber detection is 100% accurate for all flow speeds characterized. This is primarily due to the photodiode response time which is less than 1 μs. In order not to be detected, the worm needs to pass through the 125 μm fiber cross section within 1 μs which is equivalent to a speed of 125 m s^{-1}. This speed is 4–5 orders of magnitude higher than the typical operating speed in this device.

The switching results are plotted in Fig. 7(a). Worm flow speeds are measured and categorized into several groups, and in each group, we counted the number of 1) wild-type worms that exit from the correct outlet (D); 2) wild-type worms that exit from the wrong outlet (E); 3) GFP worms that exit from the correct outlet (E); and 4) GFP worms that exit from the wrong outlet (D).

Since by default the sorting device steers worms to outlet D using a pressure of 20 mbar, for our experimental configuration almost all wild-type worms exit from this outlet regardless of their flow speed. A few exceptions occurred (1 in the group of 5–7 mm s^{-1} and 3 in the group of 7–9 mm s^{-1}) when the wild-type worm entered the detection region together with a GFP worm. As a GFP signal was also detected, switching was triggered and both animals were steered to outlet E. This happened very rarely as the detection region is designed to be slightly wider than the width of a single nematode, thus allowing only one to pass through most of the time.

The switching accuracy for GFP worms was observed to reduce with increasing flow speed. For flow speeds below 7 mm s^{-1}, the sorter only made 4 mistakes. Further increasing

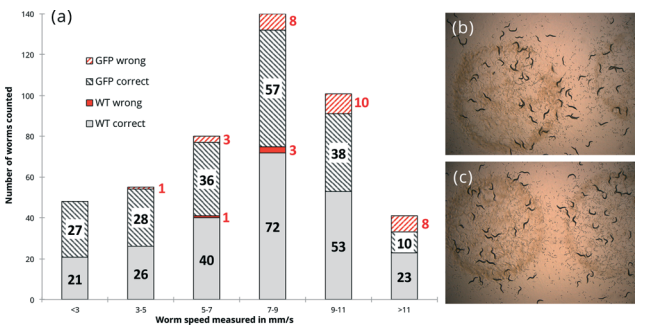

Fig. 7 (a) Sorting efficiency statistics for wild-type and GFP worms. The horizontal axis measures the speed of the worms as they pass through the sorting chip, and the vertical axis measures the number of worms counted, which is subdivided into four groups: wild-type worms that exit from the correct and wrong outlets, as well as GFP worms that exit from the correct and wrong outlets; (b–c) snapshots of CL2070 in (b) sorted and (c) control groups. Both groups of animals showed normal behavior and morphology. The large number of eggs and hatched L1 larvae can be seen in both images.

the speed will likely result in more failures because the time for nematodes to flow from the detection fibers to the switching region is shorter and the pump may not respond fast enough in some cases, especially when two nematodes flow in with a small distance interval.

At a speed of 5 mm s^{-1}, the worm takes 1 s to pass through the sorting device. If sorting speed is more favored than accuracy, it can even work at double the speed, which gives a throughput of 0.5 s per worm. Taking into consideration the time gap between one worm and another worm, the actual throughput is around 4.88 s per worm (see Video S2†) or over 700 worms per hour. This efficiency is sufficient for most real-world applications such as lifespan studies, genetic mapping and mechanistic studies.

To test if sorting by the device was harmful to nematodes, we recovered a group of sorted (switched) animals from the outlets and compared them to age-matched (day 5 of life) control animals that had not been run through the chip. We found that there were no obvious morphological or behavioral differences between switched and control animals as shown in Fig. 7(b–c). Importantly, we did not find any dead worms in either sample. Animals in both sorted and control groups began proliferating immediately, laying large numbers of eggs, which hatched into L1 larvae on the day after the experiment. We then sampled 100 adult animals randomly from each group and observed them for an additional 2 days for evidence of possible delayed, detrimental effects, such as dead or sick worms. We found that deaths in both sorted and control groups were negligible (2% over 48 h in both groups). To further test for possible sublethal stress during sorting, we ran a sample of day 5 CL2070 (dvIs70 Is[hsp-16.2::gfp; rol-6(su1006)]) animals through the system. The CL2070 strain expresses GFP under the heat-inducible HSP16.2 promoter. In case of heat shock as well as several other stressors, CL2006 nematodes express GFP, becoming fluorescent. We have used this strain previously to detect heat shock as well as activation of stress response pathways in response to drug treatment. Sorting through the device did not result in any observable fluorescence signal (data not shown), indicating the absence of stressors that would activate this stress response pathway. In particular, this confirms that animals were not exposed to stressful temperatures during sorting.

One obvious example of this lifespan study is an assay that plays a key role in a wide range of investigations in *C. elegans*.[23] Due to the time and labour intensity of daily survival scoring, such studies are typically performed with about 50–200 worms per treatment condition (*e.g.* drug dose or genotype). Even at these relatively low numbers, careful dose–response studies and independent biological repeats of lifespan studies are often not performed due to the time and effort involved. However, using the device described above in conjunction with a vital dye such as "sytox" green,[24] scoring and sorting (removal of dead animals) of 200 worms could be achieved in a short period of time, even taking handling into consideration. More importantly, unlike manual studies, the numbers can easily be scaled up to several 1000 s per condition, allowing careful dose–response studies or quantification of subtle lifespan and ageing effects that are fundamentally unobservable at lower sample numbers due to the inherent noise of lifespan studies. Finally, the fact that survival scoring in this manner does not involve manual judgment by intrinsically (unless blinded) biased operators[23] will remove observer bias, a significant and unappreciated confounder, from survival data and lifespan studies.[23]

Conclusions

In conclusion, we have presented a novel microfluidic device for high-throughput detection and sorting of the nematode *C. elegans*. In order to create an "immobilization-free" worm analysis that would not cause any potential harmful stimulus to the animals as seen in the mechanical and chemical immobilization methods, detection is achieved *via* two pairs of integrated optical fibers. Through the measurement of optical density and fluorescence, the fibers can detect and differentiate wild-type and GFP *C. elegans* worms even when they flow at high speeds. The signal is collected by photodiodes that have much shorter processing time compared to previously reported image recognition methods. At the switching region, two control inlets that only allow buffer solution to flow are integrated into the device. Fluid flow from the control inlets creates additional laminar flow fields that steer the animals to exit only from the desired outlet. By quickly changing the pressure configuration based on detected signals, switching can be achieved with a high throughput of 1 s per worm and an accuracy of more than 96%, which is suitable for most real-life studies. Based on our study, there are no accidental deaths during sorting and no significant difference in deaths between sorted and control groups following sorting.

Experimental

Fabrication of the PDMS device

The fabrication of the PDMS device was achieved using standard micromachining and soft lithography. The device was first designed in AutoCAD and exported to a laser mask writer (Heidelberg, μPG101). A chromium mask was made after the development and etching steps following laser writing for UV lithography. SU-8 2025 was spin coated on a silicon substrate at 1000 rpm to reach a thickness of 70 μm. After UV lithography and developing, the SU-8 master was then used in PDMS casting followed by 4 hours of baking. Finally, the cured PDMS was cut, punched and bound to a glass slide after plasma cleaning (Harrick Plasma, PDC-32G).

Maintaining the *C. elegans* nematodes

The Bristol N2 strain (wild type) of *Caenorhabditis elegans* (*C. elegans*) and CL2070, dvIs70 Is[hsp-16.2::gfp; rol-6(su1006)] nematodes were used in this study and were obtained from the Caenorhabditis Genetics Centre (University of Minnesota,

Minneapolis, MN). ZF1009 (kuIs29[unc-119(+) egl-13:: GFP(pWH17)]) nematodes used in this study was a kind gift from Dr. Takao Inoue (Department of Biochemistry, National University of Singapore). The worms were maintained and cultivated at 20 °C on solid nematode growth medium (NGM) (NaCl 3 g l^{-1}, bacto-agar 17 g l^{-1}, bacto-peptone 2.5 g l^{-1}, cholesterol 5 mg l^{-1}, 25 mM KPO_4 [pH 6], 1 mM $MgSO_4$ and 1 mM $CaCl_2$) seeded with streptomycin-resistant *Escherichia coli*, and OP50-1 as a food source. Preparation of NGM agar was with the addition of streptomycin at a final concentration of 200 μg ml^{-1}. Synchronous cultures of worms were obtained by hypochlorite treatment. The eggs were collected and allowed to hatch and grow on NGM plates seeded with OP50-1. Young adult (day 3 post-hatching) worms were then collected into microtubes containing M9 buffer (KH_2PO_4 3 g l^{-1}, Na_2HPO_4 6 g l^{-1}, NaCl 5 g l^{-1}, 1 mM $MgSO_4$). The worms were then washed three times in M9 buffer to remove any residual bacteria. The final pellets of worms were resuspended in 1 ml of M9 buffer until further analysis. The GFP transgenic strain (CL2070) dvIs70 Is[hsp-16.2::gfp; rol-6(su1006)] was obtained from the Caenorhabditis Genetic Centre (University of Minnesota).

Detection and sorting programming

The optical signals are detected by photodiodes (Thorlabs, DET36A/M and PerkinElmer, SPCM-AQR-14-FC) that are connected to a homemade LabVIEW program. After a small delay (calculated based on worm stream flow rate), the program triggers the pressure pump (Fluigent, MFCS-FLEX) that is connected to the same computer *via* RS-232. The pressure allocation of different channels can be pre-configured into different states, and quickly changing the states allows us to apply different pressures instantly to the buffer inlets; therefore, fast switching of worms can be achieved.

Acknowledgements

The project is supported by Singapore Institute for Neurotechnology (SINAPSE) whose sponsors include A*STAR and Mindef. We also thank the Ministry of Education, Singapore, for financial support (grant MOE2010-T2-2-048) and the Caenorhabditis Genetics Centre for the provision of worm strains.

Notes and references

1 D. L. Riddle, *C. elegans II*, 2001.
2 M. Chalfie, Y. Tu, G. Euskirchen, W. Ward and D. Prasher, *Science*, 1994, **263**, 802–805.
3 http://www.cbs.umn.edu/research/resources/cgc.
4 O. Hobert and P. Loria, in *Green Fluorescent Protein*, John Wiley & Sons, Inc., 2005, pp. 203–226.
5 T. Heidler, K. Hartwig, H. Daniel and U. Wenzel, *Biogerontology*, 2010, **11**, 183–195.
6 C. K. Leung, A. Deonarine, K. Strange and K. P. Choe, *J. Visualized Exp.*, 2011(51), 2745, DOI: 10.1039/2710.3791/2745.
7 G. Poulin, R. Nandakumar and J. Ahringer, *Oncogene*, 2004, **23**, 8340–8345.
8 E. M. Jorgensen and S. E. Mango, *Nat. Rev. Genet.*, 2002, **3**, 356–369.
9 R. Pulak, in *Methods in Molecular Biology*, ed. K. Strange, Humana Press Inc., 999 Riverview Dr, Ste 208, Totowa, NJ 07512-1165, USA, 2006, vol. 351, pp. 275–286.
10 W. A. Bonner, R. G. Sweet, H. R. Hulett and L. Herzenbe, *Rev. Sci. Instrum.*, 1972, **43**, 404–409.
11 S. E. Mango, *Nat. Biotechnol.*, 2007, **25**, 645–646.
12 Y. Duverger, J. Belougne, S. Scaglione, D. Brandli, C. Beclin and J. J. Ewbank, *Nucleic Acids Res.*, 2007, 35.
13 D. Dupuy, N. Bertin, C. A. Hidalgo, K. Venkatesan, D. Tu, D. Lee, J. Rosenberg, N. Svrzikapa, A. Blanc, A. Carnec, A. R. Carvunis, R. Pulak, J. Shingles, J. Reece-Hoyes, R. Hunt-Newbury, R. Viveiros, W. A. Mohler, M. Tasan, F. P. Roth, C. Le Peuch, I. A. Hope, R. Johnsen, D. G. Moerman, A. L. Barabasi, D. Baillie and M. Vidal, *Nat. Biotechnol.*, 2007, **25**, 663–668.
14 S. K. Sia and G. M. Whitesides, *Electrophoresis*, 2003, **24**, 3563–3576.
15 N. Chronis, M. Zimmer and C. I. Bargmann, *Nat. Methods*, 2007, **4**, 727–731.
16 S. E. Hulme, S. S. Shevkoplyas, J. Apfeld, W. Fontana and G. M. Whitesides, *Lab Chip*, 2007, **7**, 1515–1523.
17 Y. Zhang, H. Lu and C. I. Bargmann, *Nature*, 2005, **438**, 179–184.
18 J. H. Qin and A. R. Wheeler, *Lab Chip*, 2007, **7**, 186–192.
19 C. B. Rohde, F. Zeng, R. Gonzalez-Rubio, M. Angel and M. F. Yanik, *Proc. Natl. Acad. Sci. U. S. A.*, 2007, **104**, 13891–13895.
20 K. H. Chung, M. M. Crane and H. Lu, *Nat. Methods*, 2008, **5**, 637–643.
21 M. M. Crane, K. Chung and H. Lu, *Lab Chip*, 2009, **9**, 38–40.
22 T. V. Chokshi, A. Ben-Yakar and N. Chronis, *Lab Chip*, 2009, **9**, 151–157.
23 J. Gruber, L. F. Ng, S. K. Poovathingal and B. Halliwell, *FEBS Lett.*, 2009, **583**, 3377–3387.
24 M. G. Benedetti, A. L. Foster, M. C. Vantipalli, M. P. White, J. N. Sampayo, M. S. Gill, A. Olsen and G. J. Lithgow, *Exp. Gerontol.*, 2008, **43**, 882–891.

